

Establishment of Stable Cell Lines—Stable HEK293 cell lines that express miR-143 were generated by selection with 300 $\mu\text{g}/\text{ml}$ Geneticin. HEK293 cells were transfected with 0.5 μg of the pri-miR-143 expression vector at 90% confluency in 24-well dishes using a Lipofectamine LTX reagent in accordance with the manufacturer's instructions. Twelve hours after the transfection, the cells were re-plated in a 10-cm dish followed by a 3-week selection with the antibiotic. Ten surviving single colonies were picked up from each transfectant and then cultured for another 2 weeks. The cells expressing the largest amount of miR-143 among transfectants were used as miR-143 stably expressing cells.

Luciferase Reporter Assay—HEK293 cells were cultured at a density of 1×10^4 cells/well in 96-well tissue culture plates overnight, and miRNA transfections or the addition of CM was performed. The cells were harvested, and renilla luciferase activity was measured and normalized by firefly luciferase activity (10). All assays were performed in triplicate and repeated at least three times, and the most representative results are shown.

Cell Growth Assay—PC-3M-luc cells were seeded at a density of 2×10^3 cells/well in a 96-well plate. The following day the cells were transfected with mature miRNAs or incubated with a CM. Twenty-four hours later the culture medium of the transfected cells was switched to medium A, whereas the conditioned medium was not changed. After a 3-day culture, cells were harvested for the measurement of firefly luciferase activity. To know the cellular proliferation by the tetrazolium-based colorimetric MTT assay, 20 μl CM of TetraColor ONE (SEIKAGAKU Corp., Tokyo, Japan) was added to each well after 72 h of culture. After 2–4 h of incubation at 37 °C, the optical density was measured at a wavelength of 450 nm using a microplate reader.

PKH67-labeled Exosome Transfer—Purified exosomes derived from PNT-2 CM were labeled with a PKH67 green fluorescent labeling kit (Sigma). Exosomes were incubated with 2 μM PKH67 for 5 min, washed 4 times using a 100-kDa filter (Microcon YM-100, Millipore) to remove excess dye, and incubated with PC-3M-luc cells at 37 °C.

Co-culture Experiment—In co-culture experiments, 2×10^5 cells/well of PNT-2 cells were plated in 6-well plates. To stain the PNT-2 cells with BODIPY-TR-ceramide (Invitrogen), 5 μM BODIPY-TR-ceramide in a non-serum culture medium was added and incubated with the cells at 37 °C. After 30 min the cells were rinsed several times with a non-serum culture medium and incubated in a fresh medium at 37 °C for an additional 30 min. After the staining of PNT-2 cells by BODIPY-TR-ceramide, labeling of PC-3M-luc cells with PKH67 was performed in accordance with the manufacturer's instructions. After that, labeled PC-3M-luc cells were added and co-cultured with PNT-2 cells for 12 h at 37 °C.

Microarray Analysis—To detect the miRNAs in exosomes and cells derived from PNT-2 and PC-3M-luc cells, 100 ng of total RNA was labeled and hybridized using a human microRNA microarray kit (Agilent Technologies) according to the manufacturer's protocol (Protocol for Use with Agilent MicroRNA Microarrays Version 1.5). Hybridization signals were detected using a DNA microarray scanner (Agilent Tech-

nologies), and the scanned images were analyzed using Agilent Feature Extraction software.

Evaluation of Tumor-suppressive miRNA Delivery to Subcutaneously Implanted Prostate Cancer Cell Line in Mice—Animal experiments in this study were performed in compliance with the guidelines of the Institute for Laboratory Animal Research, National Cancer Center Research Institute. Seven-week-old male Balb/c athymic nude mice (CLEA Japan, Shizuoka, Japan) were anesthetized by exposure to 3% isoflurane for injections and *in vivo* imaging. Four days ahead of the first CM injection, the anesthetized animals were subcutaneously injected with 5×10^5 PC-3M-luc cells suspended in 100 μl of sterile Dulbecco's phosphate-buffered saline into each dorsal region. Five hundred μl of CM derived from miR-143-overexpressing HEK293 cells and control cells were daily injected into each tumor from day 0 to 6. For *in vivo* imaging, the mice were administered D-luciferin (150 mg/kg, Promega) by intraperitoneal injection. Ten minutes later, photons from animal whole bodies were counted using the IVIS imaging system (Xenogen) according to the manufacturer's instructions. Data were analyzed using LIVINGIMAGE 2.50 software (Xenogen).

RESULTS

Suppression of Prostate Cancer Cell Proliferation by Conditioned Medium Isolated from Non-cancerous Prostatic Cell—Cell competition is a homeostatic mechanism for the accommodation of an appropriate number of cells in a limited niche or stroma (1). Based on this idea it is possible that the cell competition between normal and abnormal cells frequently occurs in a precancerous state. Of note is that non-cancerous cells suppress cancer cell development by contact-independent interaction (12). For instance, endothelial cells provide the major extracellular heparan sulfate proteoglycan as anti-proliferative signals (12); however, the molecular mechanism by which the other types of cells in a tumor environment associate with cancer cells is not fully understood.

To analyze the mechanism, we treated a hormone-insensitive prostatic carcinoma cell line, PC-3M-luc cells, with a CM from the non-cancerous prostate cell line PNT-2 cells. After a 3-day incubation, the PNT-2 CM inhibited the growth of the PC-3M-luc cells up to ~10% compared with the cell growth treated by fresh culture medium (Fig. 1A; compare lanes 1 and 3). In contrast, the growth of PC-3M-luc cells incubated in the CM of PC-3M-luc cells themselves showed no inhibitory effect (Fig. 1A; compare lanes 1 and 2). To determine that the performed treatments did not affect the luciferase activity, we also used the colorimetric MTT assay to measure the cell growth of PC-3M-luc cells. As shown in supplemental Fig. 1A, not only luciferase assay but also MTT assay show the inhibition of PC-3M-luc cell proliferation by the addition of PNT-2 cells derived CM, indicating that our treatment did not affect the luciferase activity. These results indicate that the non-cancerous cells may secrete some molecules that can suppress cancer cell proliferation.

In a recent report we showed that miRNAs contained in exosomes are secreted and that their secretion is tightly regulated by neutral sphingomyelinase 2, which is known to hydrolyze sphingomyelins to generate ceramides and trigger the budding

Secretory miR-143 as an Anti-cancer Signal

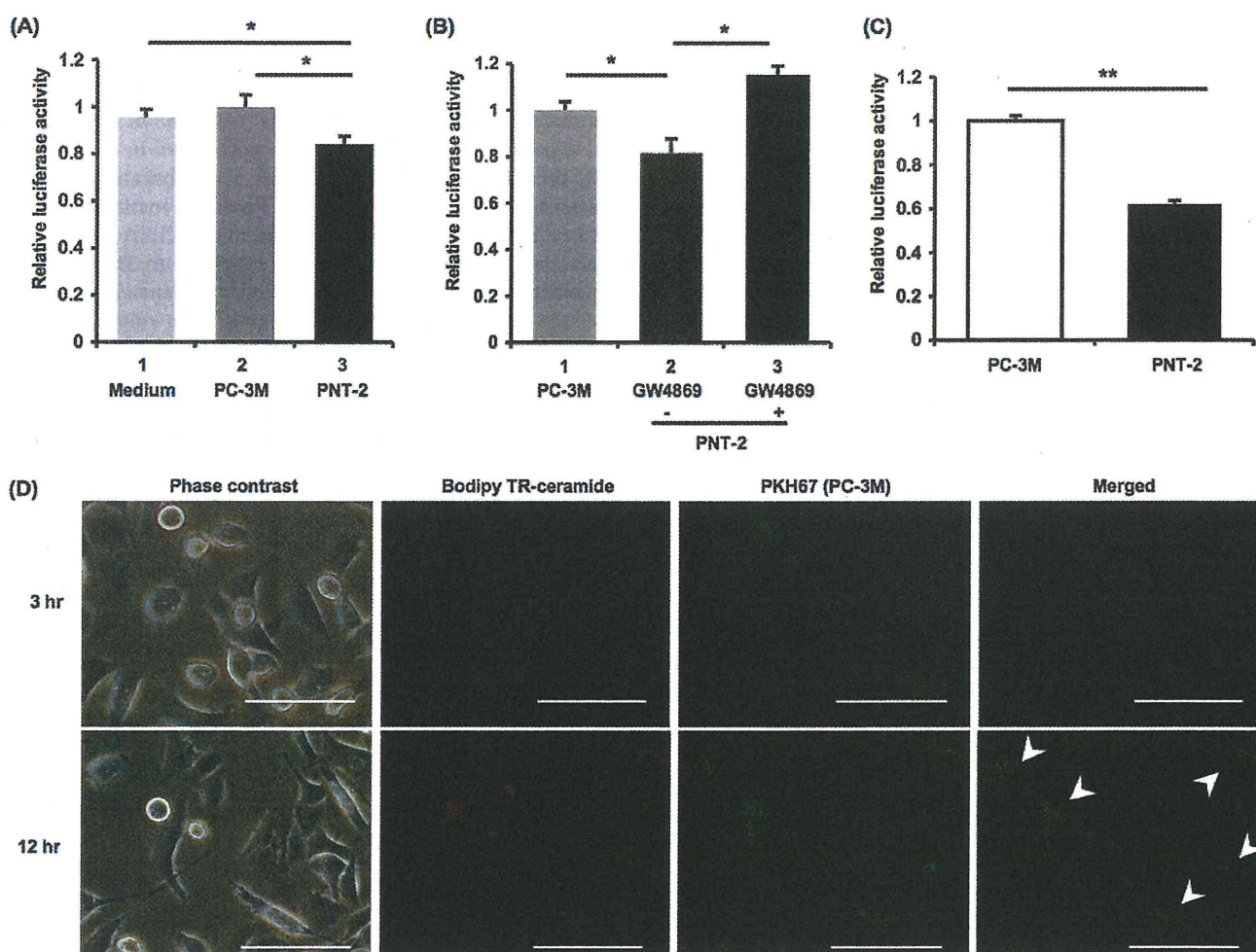


FIGURE 1. Suppression of cancerous cell proliferation by exosome isolated from non-cancerous cells. *A*, cell growth inhibition by a conditioned medium derived from PNT-2 cells is shown. PC-3M-luc cells were incubated for 3 days in a conditioned medium isolated from PC-3M-luc cells, PNT-2 cells, or a culture medium followed by a cell growth assay as described under "Experimental Procedures." The values on the y axis are depicted relative to the normalized luciferase activity of culture medium-treated cells, which is defined as 1. Each bar is presented as the mean S.E. ($n = 3$). *, $p < 0.05$ as compared with culture medium-treated PC-3M-luc cells; Student's *t* test. *B*, treatment with GW4869 to donor cells restored the reduced cell growth by the PNT-2-derived CM is shown. Donor PNT-2 cells were incubated in the presence or absence of $10 \mu\text{M}$ GW4869 for 2 days. The conditioned medium from PC-3M-luc cells was used as a control. The values on the y axis are depicted relative to the normalized luciferase activity of PC-3M-luc-conditioned medium-treated cells, which is defined as 1. Each bar is presented as the mean S.E. ($n = 3$). *, $p < 0.05$; Student's *t* test. *C*, cell growth inhibition by exosomes derived from PNT-2 cells is shown. PC-3M-luc cells were incubated in exosomes isolated from PNT-2 cells or PC-3M-luc cells followed by a cell growth assay, as described under "Experimental Procedures." The values on the y axis are depicted relative to the normalized luciferase activity of cells treated with exosomes derived from PC-3M-luc cells, which is defined as 1. Each bar is presented as the mean S.E. ($n = 3$). **, $p < 0.005$, as compared with exosomes isolated from PC-3M-luc cells; Student's *t* test. *D*, shown are fluorescent photos of BODIPY-ceramide-labeled PNT-2 and PC-3M-luc cells marked by PKH67. PNT-2 cells and PC-3M-luc cells were labeled with red fluorescent BODIPY-ceramide and green fluorescent PKH67, respectively, as described under "Experimental Procedures." After treatment of PNT-2 by BODIPY-ceramide, PKH67-labeled PC-3M-luc cells were added. After co-culturing for 3 or 12 h, images were obtained. Fluorescent photos were detected with the Eclipse TE2000 Inverted Research Microscope, and images were produced using NIS-Elements BR software. Arrowheads show yellow colored cancer cells. The size bar indicates $100 \mu\text{m}$.

of exosomes. We collected two separate aliquots of CM from PNT-2 cells incubated with or without GW4869, a specific inhibitor for neutral sphingomyelinase 2. The isolated exosomes were verified by the detection of CD63 protein, a well established exosome marker, with immunoblotting (supplemental Fig. 1B), and the activity of GW4869 was confirmed by the decreased amount of exosomal protein (supplemental Fig. 1C). The CM prepared in the presence of the GW4869 compound cancelled most tumor-suppressive activity of the non-treated PNT-2 CM (Fig. 1B; compare lanes 1–3). Furthermore, proliferation of PC-3M-luc cells was inhibited by the addition of the exosome fraction isolated from the PNT-2 CM by ultracentrifugation (Fig. 1C). These observations suggest that exo-

somal miRNAs derived from non-cancerous cells were transferred to cancerous cells, resulting in the inhibition of their proliferation.

To visualize the transfer of ceramide-containing exosome from PNT-2 to PC-3M-luc *in vitro*, a co-culture experiment was performed. Before the co-culture, 2×10^5 PNT-2 cells were incubated for 30 min with red fluorescent BODIPY-ceramide dye, which can label the exosomes inside the cells (13, 14). After washing five times with PBS, equal numbers of PC-3M-luc cells labeled by green fluorescent PKH67, a cellular membrane indicator, were added into the culture dishes. Three hours later we did not observe any PC-3M-luc cells with a yellow color (Merged photo in upper panel of Fig. 1D), indicating that car-

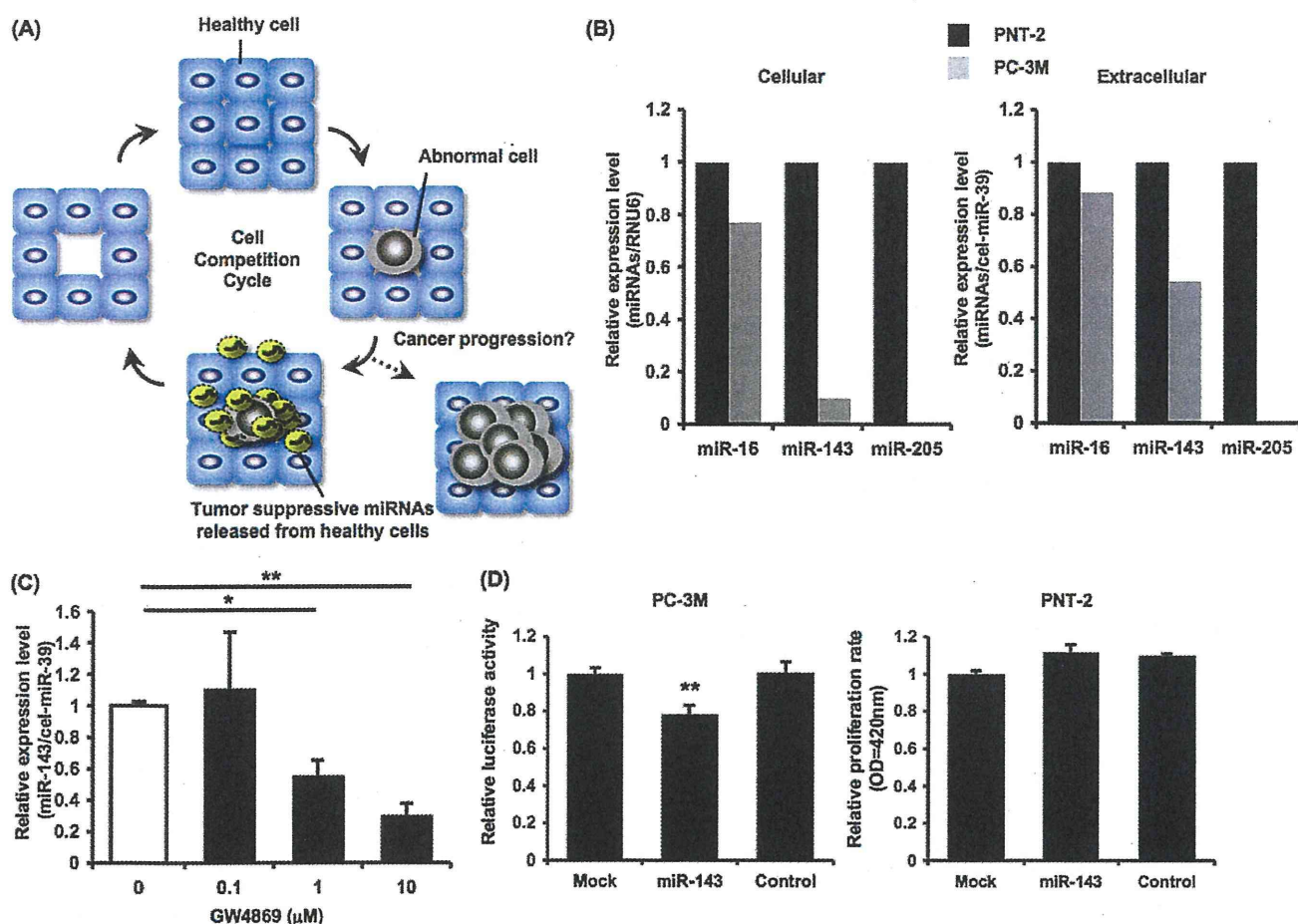


FIGURE 2. Down-regulation of cellular and extracellular tumor-suppressive miRNAs in PC-3M-luc cells. *A*, shown is a schematic representation of hypothetical tumor initiation process. Neighboring healthy cells (blue) secrete tumor-suppressive miRNAs (light yellow) to inhibit the proliferation of abnormal cells (gray), and this cell population returns to the initial healthy condition (a homeostatic cycle). Once the cell competitive cycle is compromised, this niche become susceptible to tumor initiation (indicated by a dashed arrow). *B*, comparison of cellular and extracellular miRNAs expression in PNT-2 and PC-3M-luc cells is shown. miRNA expression levels were determined by a Taq-Man QRT-PCR. The values on the y axis are depicted relative to the normalized expression level of PNT-2 cells, which is defined as 1. *C*, secretion of miR-143 was suppressed by the treatment with GW4869. PNT-2 cells were seeded and cultured in a 24-well plate for 48 h in the indicated concentrations of GW4869. After the incubation, the medium was subjected to QRT-PCR for miR-143. The values on the y axis are depicted relative to the amount of miR-143 at 0 μ M GW4869, which is defined as 1. *D*, shown is cell growth inhibition by miR-143 in PC-3M-luc cells but not in PNT-2 cells. PNT-2 and PC-3M-luc cells were transfected with 10 nM miR-143 molecules (miR-143) or 10 nM negative control molecules (control) or without RNA molecules (Mock). The values on the y axis are depicted relative to the normalized luciferase activity of untreated cells (Mock), which is defined as 1. Each bar is presented as the mean S.E. ($n = 3$). *, $p < 0.05$; **, $p < 0.005$, as compared with untreated PC-3M-luc cells; Student's *t* test.

ried-over red dyes were thoroughly removed as 3 h is enough time for the dye to be incorporated directly into the cells. By contrast, after 12 h of co-culture, yellow fluorescence was observed in green-labeled PC-3M-luc cells (indicated by arrowheads in Merged photo in the lower panel of Fig. 1D), suggesting that ceramide-containing exosomes from PNT-2 cells were transferred to the PC-3M-luc cells. This result is corroborated by the uptake experiment using the PKH67-labeled exosomes purified from PNT-2 culture medium (supplemental Fig. 1D). Green fluorescence was detected in PC-3M-luc cells after 16 h of incubation, providing a direct evidence for exosome uptake by cancerous cells.

Tumor-suppressive miRNAs Down-regulated in Cancerous Cells Were Secreted from Non-cancerous Cells—We propose a hypothetical model of tumor initiation involving cell competition and anti-proliferative secretory miRNAs (Fig. 2A). In a cell competition cycle, as illustrated in the bottom part of Fig. 2A,

growth inhibitory miRNAs are actively released from non-cancerous cells to kill abnormal cells with a partial oncogenic ability, thereby restoring them to a healthy state. Indeed, inhibitory capacity of these miRNAs appears to be limited in the setting of single treatment with the PNT-2 CM (Fig. 1A); however, they can potentially prevent emergence of tumor cells in a physiological condition. Because abundantly existing healthy cells continuously provide nascent overproliferative cells with tumor-suppressive miRNAs for a long period, a local concentration of secretory miRNAs can become high enough to restrain a tumor initiation. A dashed arrow in Fig. 2A indicates the way whereby the disruption of the homeostatic system leads to tumor expansion. If precancerous cells acquire resistance to anti-proliferative secretory miRNAs or normal cells cannot supply an adequate amount of miRNAs, then this defensive system will fail to maintain the healthy condition.

Secretory miR-143 as an Anti-cancer Signal

To test this hypothesis we checked the secretion amount of representative tumor-suppressive miRNAs by comparing PNT-2 and PC-3M-luc cells with Taq-Man QRT-PCR analysis. As shown in Fig. 2B, miR-16, miR-205, and miR-143, which are already reported to be dysregulated in prostate cancer (10, 15, 16), were down-regulated in PC-3M-luc cells at a cellular and extracellular level. The GW4869 inhibitor suppressed the secretion of miR-143 from PNT-2 cells in a dose-dependent manner (Fig. 2C), whereas its cellular level was not altered (supplemental Fig. 2A). Additionally, the application of small interfering RNAs specific for human neutral sphingomyelinase 2 gene knocked down its mRNAs, resulting in profound decrease in miR-143 secretion (supplemental Fig. 2, B and C). On the contrary, the expression of miR-143 in the cells was not changed after the transfection of neutral sphingomyelinase 2 siRNA (supplemental Fig. 2D). Taken with the result of Fig. 1B, these results suggest that the secreted tumor-suppressive miRNAs are implicated in the process of growth inhibition by PNT-2 CM.

For a global understanding of the expression change of non-cancerous and cancerous cells, we performed an miRNA microarray analysis against cellular and exosomal RNAs purified from PNT-2 and PC-3M-luc cells. In the sub-dataset of secretory exosomal miRNAs from PNT-2 cells, we found 40 miRNAs whose cellular amounts were lowered by one-half in PC-3M-luc cells (Table 1). The selected miRNAs expectedly include several types of tumor-suppressive miRNAs, such as miR-15a, miR-200 family, miR-148a, miR-193b, miR-126, and miR-205 (10, 15, 17–20). This observation supports the idea that secretory tumor-suppressive miRNAs are transferred from non-cancerous cells to cancerous cells, in accordance with the concentration gradient of the miRNA.

We have so far demonstrated that normal cells have a higher secretion of tumor-suppressive miRNAs than cancerous cells; however, it remains unclear whether or not these secreted miRNAs affect the proliferation of cells of their origin. To answer this question, we introduced synthesized miR-143 to both PNT-2 and PC-3M-luc cells and assessed their proliferation rates. After 3 days of transfections, the miR-143 analog induced growth inhibition of PC-3M-luc cells compared with mock and control small RNA transfection (Fig. 2D, left panel). In contrast, the exogenously transduced miR-143 did not show its anti-proliferative effect in PNT-2 cells (Fig. 2D, right panel), indicating that excessive miR-143 did not confer an additional growth inhibitory effect on normal cells in which expression of miR-143 is maintained to a physiological level. This finding suggests that animal cells may have their own threshold amount for miRNA activity. The different sensitivity found in different cell types can help secretory miRNAs fulfill their purpose to combat exclusively precancerous cells. It is possible that secretory miRNAs, at least, derived from non-cancerous cells such as PNT-2 cells could supplement growth-suppressive signals that are decreased in cancerous cells. Thus, secreted miR-143 might be involved in the cell competitive regulatory system.

TABLE 1

A list of PNT-2-derived secretory miRNAs that were down-regulated less than 0.5-fold in PC-3M cells compared with PNT-2 cells

miRNAs	Fold change ^a
hsa-miR-141	0.0
hsa-miR-200c	0.0
hsa-miR-886-3p	0.0
hsa-miR-30a*	0.0
hsa-miR-155	0.0
hsa-miR-205	0.0
hsa-miR-224	0.0
hsa-miR-148a	0.0
hsa-miR-130a	0.0
hsa-miR-30a	0.1
hsa-miR-663	0.1
hsa-miR-181a-2*	0.1
hsa-miR-484	0.1
hsa-miR-10a	0.1
hsa-miR-192	0.1
hsa-miR-193b	0.1
hsa-miR-200a	0.1
hsa-miR-429	0.1
hsa-miR-769-5p	0.1
hsa-miR-200b	0.2
hsa-miR-195	0.2
hsa-miR-203	0.2
hsa-miR-7	0.2
hsa-miR-200a*	0.2
hsa-miR-200b*	0.2
hsa-miR-30c	0.2
hsa-miR-126	0.3
hsa-miR-149	0.3
hsa-miR-30d	0.3
hsa-miR-181a	0.3
hsa-miR-30e*	0.3
hsa-miR-365	0.4
hsa-miR-135b	0.4
hsa-miR-454*	0.4
hsa-miR-129*	0.4
hsa-miR-30b	0.4
hsa-miR-181b	0.4
hsa-miR-210	0.4
hsa-miR-455-3p	0.5
hsa-miR-15a	0.5

^a Fold change of the expression of miRNAs in PC-3M cells compared with PNT-2 cells is indicated.

Secretory miR-143 Inhibited Prostate Cancer Cell Proliferation in Vitro—To examine whether miR-143 released from normal cells exert an anti-proliferative activity, we generated HEK293 cells overexpressing miR-143 by nearly 200-fold compared with control (supplemental Fig. 3A). After a 3-day incubation with the CM derived from the miR-143-overproducing HEK293 cells and control HEK293 cells, PC-3M-luc cells showed an ~50% decrease in proliferation (Fig. 3A, lanes 1 and 3). Importantly, the decrease was recovered by the transfection of anti-miR-143 in PC-3M-luc cells (Fig. 3A, lane 3 and 4). These data indicate that the growth inhibition is attributable to secretory miR-143 contained in the supernatant of miR-143-overexpressing HEK293 cells. In agreement with the exosome-dependent machinery of miRNA secretion, we observed a similar result by using exosome fractions purified from miR-143-transduced HEK293 cells (Fig. 3B).

To further study miRNA transfer on a molecular level, we performed a target gene expression analysis and an miRNA-responsive reporter assay. The immunoblotting analysis shows that the addition of the CM isolated from miR-143-overexpressing HEK293 cells significantly knocked down expression of KRAS, a target gene for miR-143 (21), in PC-3M-luc cells (Fig. 3C). In addition, we implemented luciferase analyses using

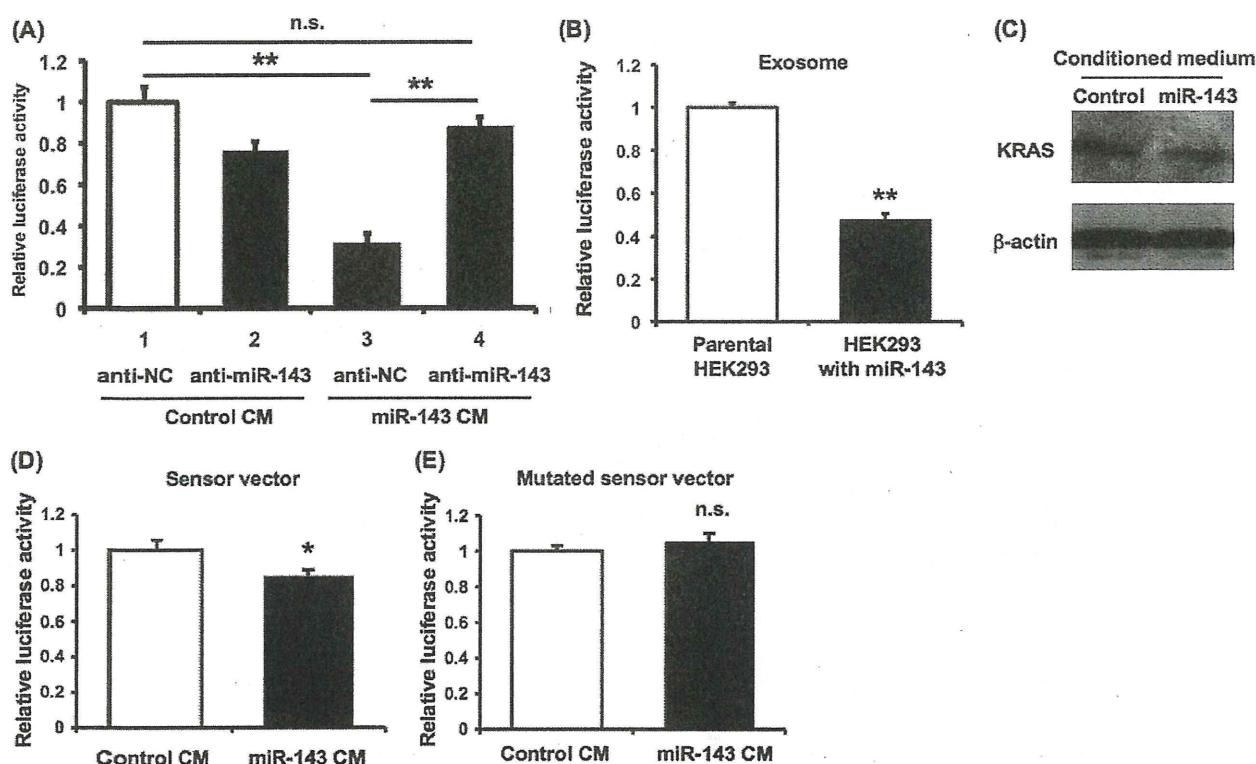


FIGURE 3. Transfer of secretory miR-143 to PC-3M-luc cells *in vitro*. *A*, the transfection of anti-miR-143 to PC-3M-luc cells restored the reduced cell growth by the CM derived from miR-143 overproducing cells. After the transfection with 3 nM miR-143 inhibitor molecule (anti-miR-143) (lanes 2 and 4) or its control molecule (anti-NC) (lanes 1 and 3), PC-3M-luc cells were incubated for 3 days in a control conditioned medium (lanes 1 and 2) and CM containing extracellular miR-143 (lane 3 and 4) followed by a cell growth assay as described under "Experimental Procedures." The values on the y axis are depicted relative to the normalized luciferase activity of cells treated in a culture medium, which is defined as 1. Each bar is presented as the mean S.E. ($n = 3$). (*, $p < 0.05$; Student's *t* test; *n.s.*, not significant). *B*, cell growth inhibition by exosomes derived from miR-143-transduced HEK293 cells is shown. PC-3M-luc cells were incubated in the exosomes followed by cell growth assay as described under "Experimental Procedures." The values on the y axis are depicted relative to the normalized luciferase activity of cells treated with exosomes derived from original HEK293 cells, defined as 1. Each bar is presented as the mean S.E. ($n = 3$). (**, $p < 0.005$; Student's *t* test). *C*, secretory miR-143-mediated KRAS suppression in PC-3M-luc cells is shown. Ten micrograms of protein of whole cell lysates prepared from PC-3M-luc cells treated with or without secretory miR-143 were applied to electrophoresis. Immunoblotting was performed with KRAS and actin antibodies and visualized by LAS-3000 system. *D*, extracellular miR-143 derived from HEK293 cells suppressed the luciferase activity of the sensor vector. HEK293 cells transfected with an miR-143 sensor vector were used as recipient cells. The recipient cells were incubated in a CM containing extracellular miRNAs. After a 2-day incubation, a luciferase reporter assay was performed as described under "Experimental Procedures." The values on the y axis are depicted relative to the normalized luciferase activity of original HEK293-conditioned medium-treated cells, which is defined as 1. Each bar is presented as the mean S.E. ($n = 3$). (*, $p < 0.05$; Student's *t* test). *E*, extracellular miR-143 did not reduce the luciferase activity of the mutated sensor vector. HEK293 cells transfected with the mutated miR-143 sensor vector were used as recipient cells. The recipient cells were incubated in a conditioned medium containing extracellular miRNAs. The luciferase assay was carried out as described above. The values on the y axis are depicted relative to the normalized renilla luciferase activity of control cells, which is defined as 1. Each bar is presented as the mean S.E. ($n = 3$). *n.s.* represents not significant.

a sensor vector harboring renilla luciferase fused in tandem with miR-143 seed sequence in the 3'-UTR. As shown in Fig. 3D, the normalized renilla luciferase activities were reduced by the treatment of miR-143-enriched CM derived from HEK293 cells stably expressing miR-143. In contrast, we did not detect any changes of luminescence by using a mutated vector instead of the intact sensor vector (Fig. 3E). Furthermore, we quantified cellular amounts of miR-143 in PC-3M-luc cells incubated with CM derived from HEK293 cells or miR-143 overproducing HEK293 cells by QRT-PCR. As shown in supplemental Fig. 3B, miR-143 was clearly increased at a cellular level by the treatment of the miR-143 enriched CM. These results indicate that secretory miR-143 exhibits its on-target growth-inhibitory effect in neighboring precancerous cells, thereby suppressing their disordered growth.

Secretory miR-143 Functions as Tumor Suppressor *in Vivo*—To our knowledge it has never been demonstrated that extracellular tumor-suppressive miRNAs can be transferred into liv-

ing cells and induce phenotypic change *in vivo*. To address this possibility, we injected CM derived from miR-143 overproducing HEK293 cells or parental HEK293 cells into nude mice implanted with PC-3M-luc cells. Four days after the subcutaneous implantation, we carried out *in vivo* imaging and CM injections according to the timetable shown in Fig. 4A. Tumor expansions have been restrained for 8 days with intratumor administrations of miR-143 enriched CM, and consequently the tumor masses shrank by ~0.5-fold on day 8 (Fig. 4B). The representative luminescent images of inoculated PC-3M-luc cells on day 8 were shown in Fig. 4C. Consistent with the finding that miR-143 did not impair growth activity of non-cancer cells *in vitro* (Fig. 2D), no toxicity was observed in these mice (data not shown). In addition, the expressions of miR-143 target genes, such as KRAS and ERK5 (16, 21), were decreased after miR-143-transduced CM injections, indicative of intercellular miRNA transfer *in vivo* (Fig. 4D). Thus, our prostate cancer xenograft model suggests that the tumor-suppressive miRNAs

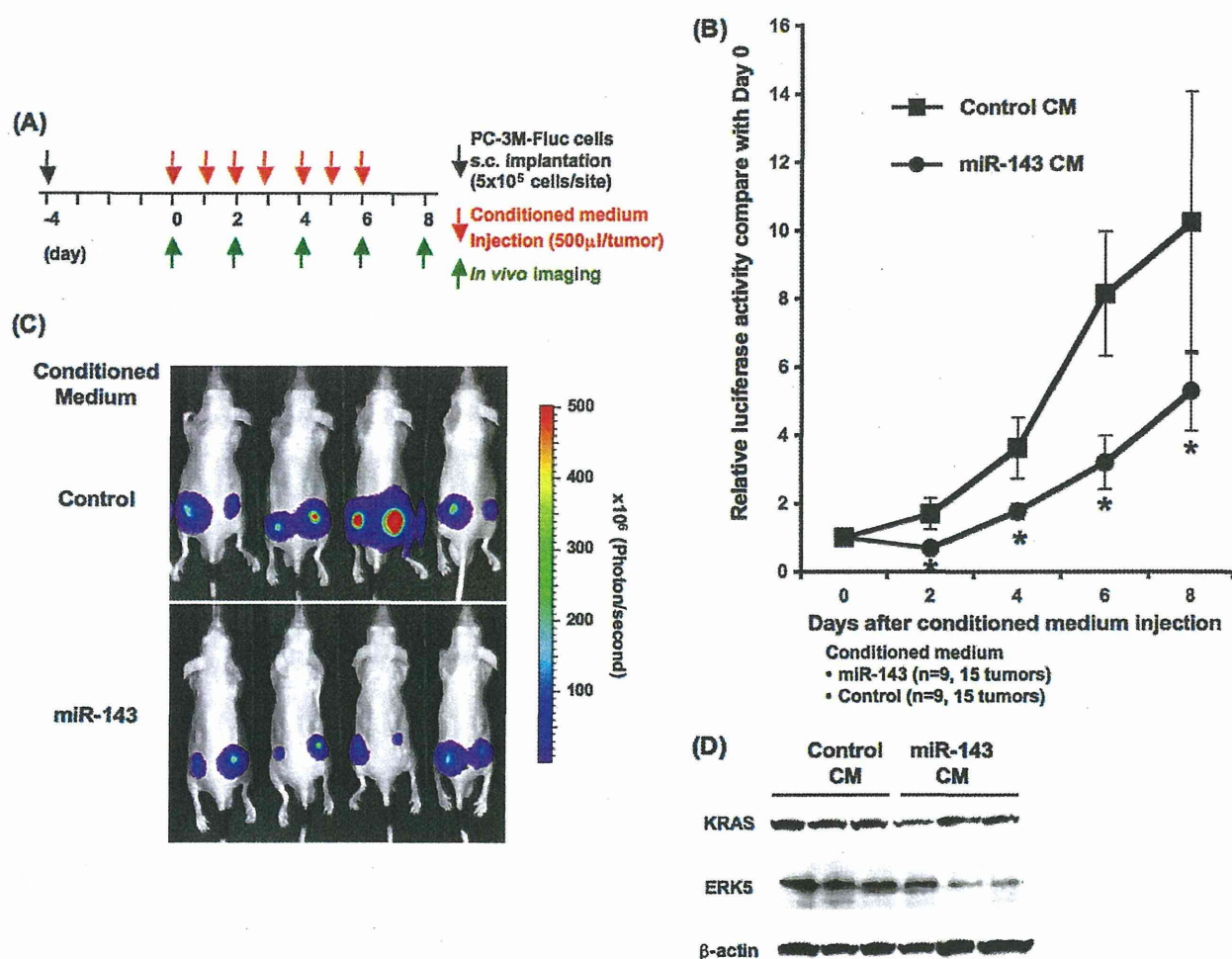


FIGURE 4. **Transfer of secretory miR-143 to PC-3M-luc cells *in vivo*.** *A*, shown is the timetable for conditioned medium injections and *in vivo* imaging. *B*, shown are tumor growth ratios of the inoculated PC-3M-luc cells during the secretory miR-143 treatment. Closed circles and closed squares indicate the tumor mass administrated with CM from miR-143-overproducing HEK293 cells or parental HEK293 cells, respectively. The values on the y axis are depicted relative to the luciferase activity of each tumor on day 0, which is defined as 1. Each bar is presented as the mean S.E. ($n = 9$). *, $p < 0.05$; Student's *t* test. *C*, representative images are shown of tumor cells in the skin of mice. Bioluminescence of firefly luciferase from miR-143-enriched CM treated mice and control mice were detected on day 8 with IVIS imaging system. *D*, shown is secretory miR-143-mediated KRAS and ERK5 suppression in inoculated tumor cells. On day 8 the inoculated tumor masses were isolated and applied to immunoblotting analysis for the quantification of KRAS and ERK5 on a protein level.

secreted from normal cells could be efficiently delivered into their neighboring tumors *in vivo*.

DISCUSSION

In this study we documented that miR-143 derived from non-cancerous cells had the ability to suppress the growth of cancer cell proliferation not only *in vitro* but also *in vivo*. These observations suggest that tumor-suppressive miRNAs can be implicated in cell competition between cancer cells and non-cancer cells. In this context, normal cells attempt to prevent the outgrowth of precancerous cells by secreting anti-proliferative miRNAs and maintain a healthy condition; however, the abnormal cells can circumvent this inhibitory machinery, finally resulting in a tumor expansion (Fig. 2A). Cell competition could be a homeostatic mechanism that tumor cells need to overcome (1).

Here, we discuss two possible mechanisms by which cancer cells can gain resistance to secretory tumor-suppressive miRNAs. One is a blockade for the uptake of miRNAs, and the

other is a cancellation of silencing activity of the incorporated miRNAs. As previously reported, miRNAs are loaded into exosomes and then secreted from living cells (7, 22, 23). If exosomes enriched in miRNAs are actively incorporated by recipient cells, cancer cells can impair the uptake mechanism to escape from the attack of secretory tumor-suppressive miRNAs. This scenario is supported by a recent publication regarding a Tim4 expected for an exosome receptor (24).

In the latter case cancer cells need to specifically compromise the incorporated tumor-suppressive miRNAs because there are some types of miRNAs that are indispensable for the expansion of cancer cells. A RISC assembly is composed of many protein families, such as the mammalian AGO family, GW182, and heat shock proteins (25). Moreover, each gene family also consists of many members, thereby generating diversity of RISC assemblies. The heterogeneity of RISC assemblies allows tumor-suppressive miRNAs to selectively bind with a RISC and silence their target genes on the complex. If cancer cells can exclusively destroy the tumor-suppressive RISC assembly, they can safely

grow in a limited niche full of anti-proliferative miRNAs. The detailed mechanism of the resistance to cell competition remains unknown.

In addition to the acquired resistance, there is another possibility that normal cells will lose secretory capacity of exosomal miRNAs. p53 was shown to enhance exosome production in cells undergoing a p53 response to stress (26). In other words, dysfunction of p53 will result in decreased miRNA secretion. The tumor-suppressive ability of p53 can partly depend on the control of miRNA release from normal cells.

Numerous studies show a broad variety of reasons for tumor initiation, including gene amplification, cellular stress, metabolic alteration, and epigenetic changes. This work suggests that the disruption of the cell competitive process mediated by secretory miRNAs will result in the occurrence of neoplasm. Understanding the mechanism by which homeostasis is impaired leads to a novel therapeutic approach for cancer progression.

Acknowledgments—We thank Katsuyuki Hayashi and Ikuei Hiraka at DNA Chip Research Inc. for supporting the processing of microarray data. We thank Ayako Inoue for excellent technical assistance.

REFERENCES

- Johnston, L. A. (2009) Competitive interactions between cells: death, growth, and geography. *Science* **324**, 1679–1682
- Díaz, B., and Moreno, E. (2005) The competitive nature of cells. *Exp. Cell Res.* **306**, 317–322
- Hanahan, D., and Weinberg, R. A. (2011) Hallmarks of cancer. The next generation. *Cell* **144**, 646–674
- Bondar, T., and Medzhitov, R. (2010) p53-mediated hematopoietic stem and progenitor cell competition. *Cell Stem Cell* **6**, 309–322
- Dong-Le Bourhis, X., Berthois, Y., Millot, G., Degeorges, A., Sylvi, M., Martin, P. M., and Calvo, F. (1997) Effect of stromal and epithelial cells derived from normal and tumorous breast tissue on the proliferation of human breast cancer cell lines in co-culture. *Int. J. Cancer* **71**, 42–48
- Senoo-Matsuda, N., and Johnston, L. A. (2007) Soluble factors mediate competitive and cooperative interactions between cells expressing different levels of *Drosophila* Myc. *Proc. Natl. Acad. Sci. U.S.A.* **104**, 18543–18548
- Kosaka, N., Iguchi, H., Yoshioka, Y., Takeshita, F., Matsuki, Y., and Ochiya, T. (2010) Secretory mechanisms and intercellular transfer of microRNAs in living cells. *J. Biol. Chem.* **285**, 17442–17452
- Croce, C. M. (2009) Causes and consequences of microRNA dysregulation in cancer. *Nat. Rev. Genet.* **10**, 704–714
- Suzuki, H. I., Yamagata, K., Sugimoto, K., Iwamoto, T., Kato, S., and Miyazono, K. (2009) Modulation of microRNA processing by p53. *Nature* **460**, 529–533
- Takeshita, F., Patrawala, L., Osaki, M., Takahashi, R. U., Yamamoto, Y., Kosaka, N., Kawamata, M., Kelnar, K., Bader, A. G., Brown, D., and Ochiya, T. (2010) Systemic delivery of synthetic microRNA-16 inhibits the growth of metastatic prostate tumors via down-regulation of multiple cell-cycle genes. *Mol. Ther.* **18**, 181–187
- Peng, X., Guo, W., Liu, T., Wang, X., Tu, X., Xiong, D., Chen, S., Lai, Y., Du, H., Chen, G., Liu, G., Tang, Y., Huang, S., and Zou, X. (2011) Identification of miRs-143 and -145 that is associated with bone metastasis of prostate cancer and involved in the regulation of EMT. *PLoS One* **6**, e20341
- Franses, J. W., Baker, A. B., Chitalia, V. C., and Edelman, E. R. (2011) *Sci. Transl. Med.* **3**, 66ra65
- Savina, A., Vidal, M., and Colombo, M. I. (2002) The exosome pathway in K562 cells by Rab11. *J. Cell Sci.* **115**, 2505–2515
- Trajkovic, K., Hsu, C., Chiantia, S., Rajendran, L., Wenzel, D., Wieland, F., Schwille, P., Brügger, B., and Simons, M. (2008) Ceramide triggers budding of exosome vesicles into multivesicular endosomes. *Science* **319**, 1244–1247
- Gandellini, P., Folini, M., Longoni, N., Pennati, M., Binda, M., Colecchia, M., Salvioni, R., Supino, R., Moretti, R., Limonta, P., Valdagni, R., Daidone, M. G., and Zaffaroni, N. (2009) miR-205 exerts tumor-suppressive functions in human prostate through down-regulation of protein kinase Cepsilon. *Cancer Res.* **69**, 2287–2295
- Clapé, C., Fritz, V., Henriquet, C., Apparailly, F., Fernandez, P. L., Iborra, F., Avancès, C., Villalba, M., Culine, S., and Fajas, L. (2009) miR-143 interferes with ERK5 signaling and abrogates prostate cancer progression in mice. *PLoS One* **4**, e7542
- Kong, D., Li, Y., Wang, Z., Banerjee, S., Ahmad, A., Kim, H. R., and Sarkar, F. H. (2009) miR-200 regulates PDGF-D-mediated epithelial-mesenchymal transition, adhesion, and invasion of prostate cancer cells. *Stem Cells* **27**, 1712–1721
- Fujita, Y., Kojima, K., Ohhashi, R., Hamada, N., Nozawa, Y., Kitamoto, A., Sato, A., Kondo, S., Kojima, T., Deguchi, T., and Ito, M. (2010) MiR-148a attenuates paclitaxel resistance of hormone-refractory, drug-resistant prostate cancer PC3 cells by regulating MSK1 expression. *J. Biol. Chem.* **285**, 19076–19084
- Saito, Y., Friedman, J. M., Chihara, Y., Egger, G., Chuang, J. C., and Liang, G. (2009) Epigenetic therapy up-regulates the tumor suppressor microRNA-126 and its host gene EGFL7 in human cancer cells. *Biochem. Biophys. Res. Commun.* **379**, 726–731
- Rauhala, H. E., Jalava, S. E., Isotalo, J., Bracken, H., Lehmusvaara, S., Tammele, T. L., Oja, H., and Visakorpi, T. (2010) miR-193b is an epigenetically regulated putative tumor suppressor in prostate cancer. *Int. J. Cancer* **127**, 1363–1372
- Xu, B., Niu, X., Zhang, X., Tao, J., Wu, D., Wang, Z., Li, P., Zhang, W., Wu, H., Feng, N., Wang, Z., Hua, L., and Wang, X. (2011) miR-143 decreases prostate cancer cells proliferation and migration and enhances their sensitivity to docetaxel through suppression of KRAS. *Mol. Cell Biochem.* **350**, 207–213
- Gibbins, D. J., Ciaudo, C., Erhardt, M., and Voinnet, O. (2009) Multivesicular bodies associate with components of miRNA effector complexes and modulate miRNA activity. *Nat. Cell Biol.* **11**, 1143–1149
- Pegtel, D. M., Cosmopoulos, K., Thorley-Lawson, D. A., van Eijndhoven, M. A., Hopmans, E. S., Lindenberg, J. L., de Gruijl, T. D., Würdinger, T., and Middeldorp, J. M. (2010) Functional delivery of viral miRNAs via exosomes. *Proc. Natl. Acad. Sci. U.S.A.* **107**, 6328–6333
- Miyaniishi, M., Tada, K., Koike, M., Uchiyama, Y., Kitamura, T., and Nagata, S. (2007) Identification of Tim4 as a phosphatidylserine receptor. *Nature* **450**, 435–439
- Kwak, P. B., Iwasaki, S., and Tomari, Y. (2010) The microRNA pathway and cancer. *Cancer Sci.* **101**, 2309–2315
- Yu, X., Harris, S. L., and Levine, A. J. (2006) The regulation of exosome secretion. A novel function of the p53 protein. *Cancer Res.* **66**, 4795–4801

Gene-manipulated embryonic stem cells for rat transgenesis

Masaki Kawamata · Takahiro Ochiya

Received: 1 January 2011 / Revised: 3 March 2011 / Accepted: 10 March 2011 / Published online: 25 March 2011
© Springer Basel AG 2011

Abstract Embryonic stem cells (ESCs) are derived from blastocysts and are capable of differentiating into whole tissues and organs. Transplantation of ESCs into recipient blastocysts leads to the generation of germline-competent chimeras in mice. Transgenic, knockin, and knockout gene manipulations are available in mouse ESCs, enabling the production of genetically modified animals. Rats have important advantages over mice as an experimental system for physiological and pharmacological investigations. However, in contrast to mouse ESCs, rat ESCs were not established until 2008 because of the difficulty of maintaining pluripotency. Although the use of signaling inhibitors has allowed the generation of rat ESCs, the production of genetically modified rats has been difficult due to problems in rat ESCs after gene introduction. In this review, we will focus on some well-documented examples of gene manipulation in rat ESCs.

Keywords ES cell · Rat · Transgenic · Pluripotency · Chimera

Introduction

Embryonic stem cells (ESCs) established from the inner cell mass (ICM) of preimplantation blastocysts [1] have been routinely derived from mice since 1981 [2, 3]. These cells have a stable developmental potential to form derivatives of all three embryonic germ layers, the endoderm,

mesoderm, and ectoderm, even after prolonged culture [4] and have been used to study the mechanism of cell differentiation. Moreover, they are capable of generating germline chimeras following injection into the blastocyst [5]. Gene manipulation is available, and germline transmission of transgenic ESCs was achieved in 1986 [6]. Soon after this achievement was reported, gene-targeting mice were generated via homologous recombination in ESCs [7]. So far, a huge number of genetically modified mice have been produced via the manipulation of ESCs and used in a range of biomedical researches. However, this technique is unavailable in species other than mice because of a lack of stable ESCs.

The laboratory rat, the first mammalian species domesticated for scientific research, has been used as an animal model for research in physiology, toxicology, nutrition, behavior, immunology, and neoplasia for over 150 years [8–12]. Despite the utility to use rats in experiments, rat ESCs were not established until 2008. The reasons for the failure to develop ESCs in rats are related to the difficulty in maintaining pluripotency in culture despite trials using numerous strategies [13–17]. Our group generated rat ESCs harboring a potential to contribute to chimera but not to develop germ cells [18]. On the other hand, despite the lack of authentic ESCs, several technologies have been developed to alter rats genetically [19–26].

Rat transgenesis from ESCs with 2i+LIF medium

In 2008, germline-competent rat ESCs were first established from blastocysts by using a 2i+LIF medium composed of two signaling inhibitors (MEK inhibitor PD0325901; GSK3 inhibitor CHIR99021), a leukemia inhibitory factor (LIF), and a defined basal culture medium

M. Kawamata · T. Ochiya (✉)
Division of Molecular and Cellular Medicine,
National Cancer Center Research Institute, 1-1,
Tsukiji, 5-chome, Chuo-ku, Tokyo 104-0045, Japan
e-mail: tochiya@ncc.go.jp

containing no fetal bovine serum (FBS) (Fig. 1) [27, 28]. The results of the two studies showed that FBS was a key factor in the induction of differentiation in rat ESCs [29]. This culture medium was also used for the generation of mouse ESCs [30]. Generally, mouse ESCs are cultured on feeder layers of mouse embryonic fibroblasts (MEFs). Further, it was found that the use of DIA-M cells [27] or a mixture of MEFs and L-cells as feeder layers [28] was optimal for isolating rat ESCs. In these conditions, although ESCs maintained pluripotency and contributed to chimeras, only two of nine cell lines achieved germline transmission. Rat-induced pluripotent stem cells (iPSCs) with the potential to contribute to chimeras were also generated by the addition of A-83-01 (Type 1 Tgf β receptor inhibitor) to 2i+LIF in a mouse ESC basal culture medium containing 20% knockout serum replacement (KSR). However, these iPSCs did not achieve germline transmission [31].

Gene introduction was available in the rat ESCs cultured in 2i+LIF medium. However, they were sensitive to electro-physical stimulation induced by the conventional electroporation method, which led to cell death. A nucleofection method was found to be more efficient and convenient for gene introduction in rat ESCs [28]. Furthermore, FBS was temporally added into an electroporation medium as well as a 2i+LIF cell-culture medium to aid viability [27]. Each group obtained stable transfectant clones in which the CAG-eGFP-IRES-pac plasmid was randomly integrated in their genome after selection with puromycin [27, 28]. Although five overt coat color chimeras were born after injection of the clone, they either died perinatally or were euthanized due to jaw abnormalities. The reasons for their abnormalities might have been chromosomal instability in the transfectant ESC line [27]. On the other hand, Hirabayashi et al. [32] succeeded in the germline transmission of a transfectant rat ESC line

harboring a humanized Kusabira-Orange (huKO) gene using the 2i+LIF culture medium. A CAG/huKO-neo plasmid was introduced into ESCs by electroporation, and then stable clones were obtained by neomycin selection. In the 2i+LIF medium, 1,000 U/ml of rat LIF [33] was substituted for the human LIF used in the previous works (100 U/ml [27]; 10 U/ml [28]). It is possible that the rat LIF is better for the maintenance of rat ESCs [34]. Kobayashi et al. [35] overcame the difficulty to generate interspecific chimeras between rats and mice using rat ES or iPS cells cultured in a 2i+rat LIF medium. Thus, using rat LIF might be an option to keep rat ESCs stable.

Rat transgenesis from ESCs with YPAC medium

Our group developed a new culture medium (YPAC medium) including the additional signaling inhibitors of Rho-associated kinase (Y-27632) and A-83-01 to the 2i [36]. The four inhibitors, Y-27632, PD0325901, A-83-01, and CHIR99021, are collectively referred to as YPAC. A mouse ESC basal culture medium containing FBS (20% vol/vol) and MEFs was used, but LIF was not necessary in our study (Fig. 1). In the culture condition, the majority of cell lines (six out of six) demonstrated chimerism and germline transmission and could be stably transfected with a reporter transgene to produce genetically modified rats. These three cell lines were derived from each of the following strains: Wistar, LEA (Long Evans Agouti), and hybrid Wistar/LEA [36].

Since the medium contained 20% serum, the ESCs were tolerant to the damage induced by electric stimuli during gene introduction. In our procedure, a transgene in which the Venus gene was transcribed by the *Oct4*-promoter (*Oct4*-Venus) was introduced in the ESCs by the nucleofection method. When the manipulated cells were plated,

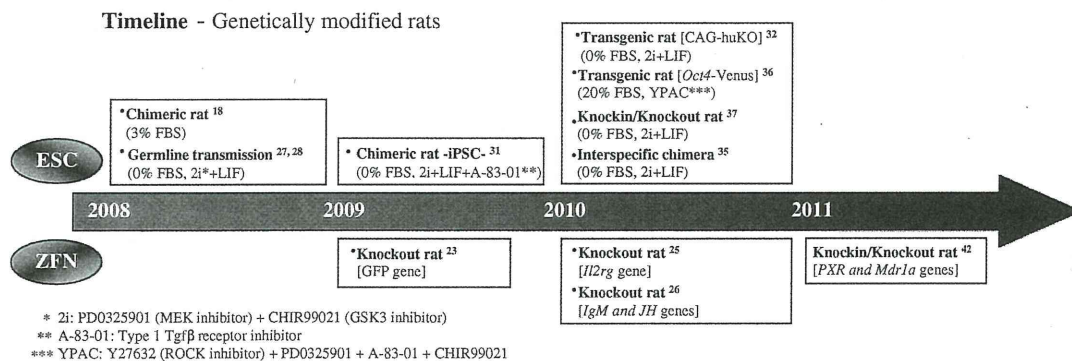


Fig. 1 Timeline of rat transgenesis using ESC or ZFN technology since 2008. The *parentheses* indicate the culture conditions. The *brackets* indicate transgenes or targeted genes

the use of matrigel (2% at final concentration) was effective for selecting stable clones because they are retained to adhere on MEFs [36]. It is generally known that rat ESC colonies tend to detach from MEFs [27, 28, 36]. This phenomenon enhances the ESCs' attachment to each other, leading to clone contamination. As the transgene did not include a selection cassette, Venus-positive clones were picked and expanded without drugs. In this cloning process, we found an advantage of using ESCs for the generation of transgenic rats because we were able to choose high-quality clones mimicking an endogenous *Oct4* expression pattern. While the majority of the clones exhibited a heterogeneous expression pattern in undifferentiated cells, only a few clones maintained homogenous expression after long-term culture (Fig. 2a). This homogeneity corresponds to the expression pattern of endogenous OCT4 protein. *Oct4*-Venus transgenic rats were generated through germline transmission of the selected clones without any adverse effects of gene introduction on chimera contribution (Fig. 2b). The Venus fluorescence was also detected in germ cells of the transgenic fetal gonads (Fig. 2c). Moreover, we could trace the fluorescence only in undifferentiated ESCs from their blastocysts during the establishment process and long-term culture (Fig. 2d) [36].

Gene targeting rats from ESCs

Tong et al. [37] achieved for the first time the production of knockout rats via homologous recombination in rat ESCs. A targeting vector was constructed to disrupt the tumor suppressor gene *p53* (also known as *Tp53*). Targeting efficiencies in two ESC lines derived from the DA (Dark Agouti) strain were 1.12–3.70%. Many properly targeted cell lines cultured in the 2i+LIF medium developed chromosome abnormalities. Over 65% of the cells were polyploid. This phenomenon is similar to that reported in previous works [27, 28]. However, after subcloning round and compact colonies, two out of 20 clones had euploid chromosome numbers leading to the production of a viable knockout [34]. This achievement is historic because the *p53* knockout rat validates the culminated effort of many to enable targeted genetic engineering in rat ESCs. Another group also succeeded in gene targeting in a hypoxanthine phosphoribosyltransferase (*hprt*) locus by homologous recombination in rat ESCs [38]. Although these *hprt* heterozygous clones cultured in the 2i+LIF medium maintained pluripotency, aneuploid cells did emerge in the cultures. However, approximately 2% of geneticine-resistant colonies achieved recombination correctly. The efficiency was similar to that originally reported for mouse

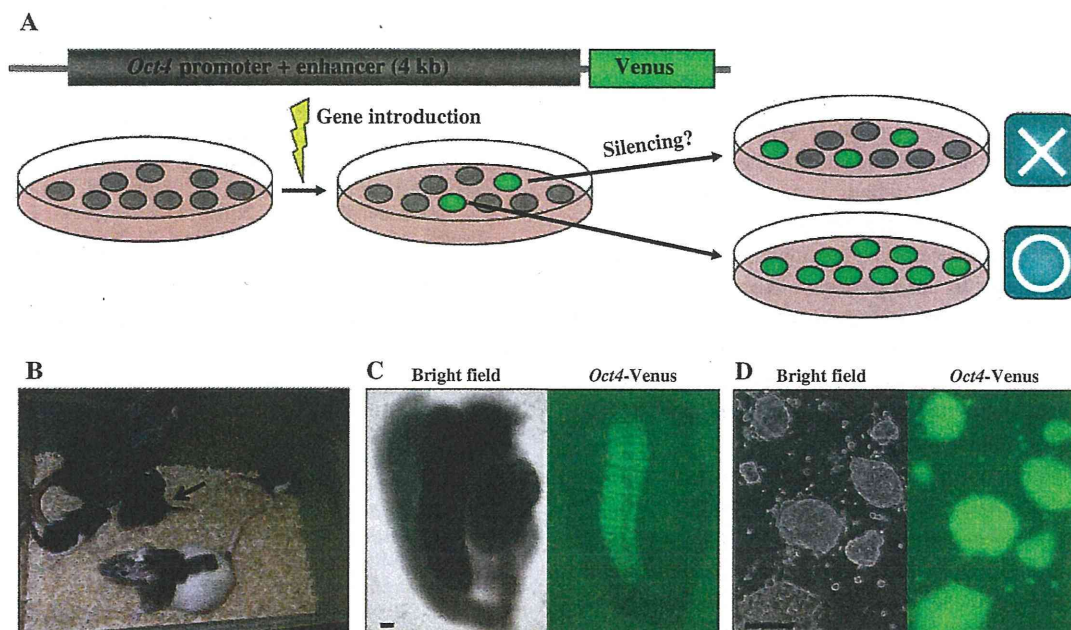


Fig. 2 Transgenesis in rat ESCs. **a** *Oct4*-Venus transgene is introduced in rat ESCs by a nucleofection method. Some clones receive random integration of the transgene, with subsequent green fluorescence. After subcloning and passaging, Venus fluorescence was decreased in a majority of the clones (*upper*), while a minority of the clones expressed the fluorescence homogeneously. **b** The *Oct4*-Venus

transgenic rat (*arrow*) was produced through germline transmission of the recombinant ESCs from a chimeric rat. **c** *Oct4*-Venus positive-germ cells in E16.0 gonad of the transgenic rats. **d** An ESC line derived from the *Oct4*-Venus transgenic rat. Venus fluorescence was kept in undifferentiated cells after 18 passages. All scale bars, 100 μ m